Journal of Photochemistry and Photobiology A: Chemistry 222 (2011) 111–116

Contents lists available at ScienceDirect

Journal of Photochemistry and Photobiology A: Chemistry

journal homepage: www.elsevier.com/locate/jphotochem

Kinetic and efficiency of TiO_2-coated on foam or tissue and TiO_2-suspension in a photocatalytic reactor applied to the degradation of the 2,4-dichlorophenol

G. Plantard [a,b,*], F. Correia [a], V. Goetz [a]

[a] PROMES-CNRS, UPR 8521, PROcédés Matériaux et Energie Solaire, Rambla de la Thermodynamique, Technosud, 66100 Perpignan cedex, France
[b] Université de Perpignan Via Domitia 52 avenue Paul Alduy, 66860 Perpignan, France

ARTICLE INFO

Article history:
Received 4 February 2011
Received in revised form 11 May 2011
Accepted 21 May 2011
Available online 27 May 2011

Keywords:
TiO_2
Foam
Yield
Photocatalysis

ABSTRACT

In the field of advanced oxidization processes based on solar radiation, heterogeneous solar catalysis involves exciting a photocatalyst with UV rays and one of the major problems encountered is optimizing the use of the sunlight. The work presented here aimed to use an efficient material able to provide a high active specific surface expressed in square meter per unit volume of the reactor. Recently, macroporous reticulated materials such as foams have been utilized as substrates in heterogeneous catalysis on account of their uniform cellular structure. Thanks to their macroscopic arrangement, they provide a large interface for exchange between the targeted molecules and the solar radiation. The reactor in which the degradation kinetics were observed was a cylindrical borosilicate glass tube operated in a recirculation batch mode. The measurement of the degradation kinetics was carried out on a model target molecule, 2,4 dichlorophenol, at an initial concentration of 20 mg l^{-1}. The effects of photolysis, output flow and the intensity of the radiation were studied. The results were treated using a first order kinetic law according the TOC concentration. It emerges that the rate of degradation is related exclusively to the quantity of light absorbed. For each material, the efficiency of the material was independent of the intensity of the radiation received. In this context, macroporous reticulated materials such as foams show promise as supports for photocatalysts.

1. Introduction

Solar detoxification is an outstanding demonstration of how well suited solar energy is to environmental conservation and can be employed with complex mixtures of contaminants [1,2]. This enhanced oxidization process enables species resistant to bioprocesses to be broken down and finally, in ideal cases, mineralized into CO_2 and water [1–3]. In the field of advanced oxidization processes based on solar radiation, heterogeneous solar catalysis involves exciting a photocatalyst with UV rays and the major problem encountered is optimizing the use of the sunlight. The ultra violet region, including A-B, corresponds to only 5% of the total available solar flux reaching the surface of the earth. This represents a maximum irradiation available for the solar catalytic process of 50 W_{UV} m^{-2} (Fig. 1). Special focus and effort needs to be given to the use of solar radiation in the ultraviolet range as well as to the efficiency of each material as a function of the intensity of the solar radiation. Hence the importance of developing innovative materials effective in harnessing and using sunlight [4–7].

In this context, the work presented here aimed to use an efficient material able to provide a high active specific surface expressed in square meter per unit volume of the reactor. Recently, macroporous reticulated materials such as foams have been utilized as substrates in heterogeneous catalysis on account of their uniform cellular structure [4–9]. Thanks to their macroscopic arrangement, they provide a large interface for exchange between the targeted molecules and the solar radiation. Such materials would appear promising as a support for photocatalysts [6–9]. The aim was thus to ascertain the effect of two- and three-dimensional structures on the ability of a material to use light rays and, thereafter, to assess the apparent quantum yield of the materials used. To this end, in the first part of the investigation, the sol–gel method designed by Addamo [10] was optimized to obtain enhanced reactivity of the materials used. The reactivity of each material was then determined in various conditions of radiation so as to establish the correlation between the kinetics of photodegradation, the structure of the material and the intensity of the radiation. Finally, the apparent quantum yield for the different materials is presented as a way of defining and comparing their capacity to degrade pollutants.

* Corresponding author at: PROMES-CNRS, UPR 8521, PROcédés Matériaux et Energie Solaire, Rambla de la Thermodynamique, Technosud, 66100 Perpignan cedex, France. Tel.: +33 61 25 24 782; fax: +33 4 68 68 22 13.
E-mail address: plantard@univ-perp.fr (G. Plantard).

1010-6030/$ – see front matter © 2011 Elsevier B.V. All rights reserved.
doi:10.1016/j.jphotochem.2011.05.009

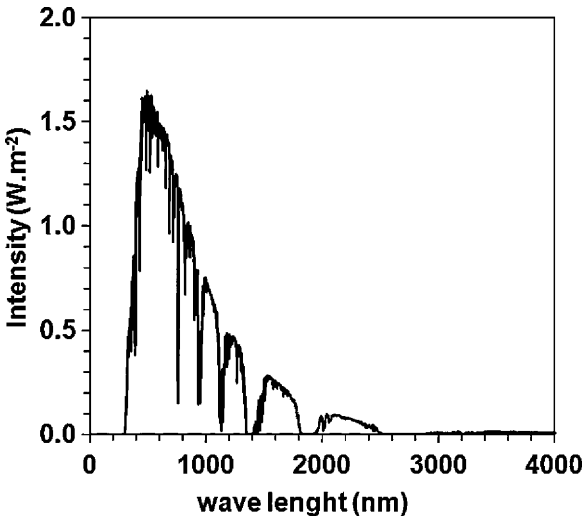

Fig. 1. Solar spectrum (AM1.5) representing the incident flux (scattered and direct) throughout the whole range of wavelengths.

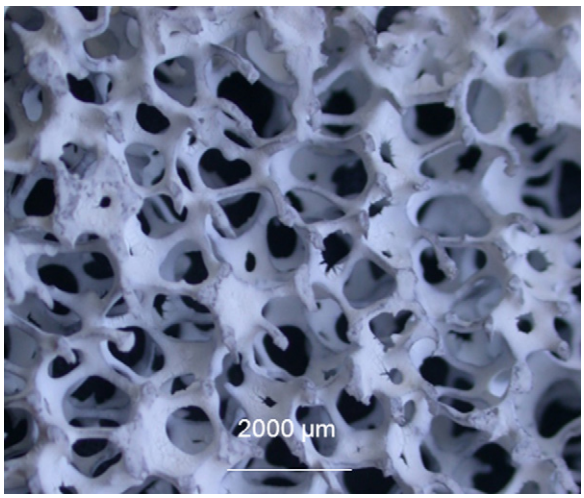

Fig. 2. Photographs taken with the scanning electron microscope of a foam constituted by cavities and meshes (mesh diameter of 2 mm).

2. Experimental

2.1. Chemicals and materials

The 2,4-dichlorophenol (2,4-DCP) was selected as the pollutant organic molecule. Much work has been done on the 2,4-DCP, a chemical compound commonly used in many industrial applications [11].

The catalyst was TiO_2, the material most widely used for photocatalysis. In this study, three materials, each possessing different properties, were investigated: a powder supplied by Degussa (P-25), a cellulose support impregnated with TiO_2 made by the Ahlstrom company and, also, a foam made in the laboratory then coated with TiO_2. P-25 was taken as the reference material on account of its photocatalytic behaviour. Its specific surface area (BET) was $54\,m^2\,g^{-1}$ and the particles of TiO_2 had an average diameter of about 20 nm. The photocatalytic material provided by Ahlstrom consisted of TiO_2 (Millenium PC-500) immobilized on a flat and flexible non-woven support of cellulose fibers (paper grade 1048). Its specific surface area referenced with the total photocatalytic material mass was equal to $98\,m^2\,g^{-1}$. More precisely, this photocatalytic material consisted of cellulosic fibers ($38\,g\,m^{-2}$), TiO_2 ($16.7\,g\,m^{-2}$), zeolite ($2\,g\,m^{-2}$) and SiO_2 ($13.3\,g\,m^{-2}$). A reticulated metallic foam with high porosity was used as the third support material for the photocatalyst (Fig. 2). This original material provides a variable architecture depending on the size of the mesh and the holes making it up [7]. The aluminium foam support for the coating of TiO_2 had a density of $0.2\,g\,cm^{-3}$ porosity around 95% and had the following structure: mesh wall thickness 0.75 mm, mesh hole diameter 2 mm.

2.2. Synthesis of the catalyst

The synthesising protocol designed by Addamo [10] was adapted for the purpose of depositing a thin coat of TiO_2 on the foam. A further requirement was to endow the supports with good bonding characteristics in order to ensure that the TiO_2 adhered to its support. The surface of the media was first treated chemically with fluorohydric acid at 5%. Silica was then put on using the classic sol–gel method [10], providing a surface favorable to the adhesion of the TiO_2 deposit. The inorganic polymerization of the silica was started off with the TEOS precursor. The solution was stirred for 2 h in an inert atmosphere (N_2). This gel was subsequently applied to the scaffold media by dip-coating. After each SiO_2 coating, the new layer was dried for 5 min at 373 K and then calcined at 573 K for 3 h. This coating process was repeated three times.

It has been shown recently that the properties of TiO_2–SiO_2 composites, when in nano-form, considerably enhance the properties of the coating on the surface of the support material [12]. But, the presence of a binder affects the photocatalytic efficiency [13]. We suggest to use a deposit performed with a TiO_2 powder disperse in a sol–gel made of silica. A preliminary study was addressed [14] to determine the right balance between reactivity and bonding as a function of the masses of catalyst (TiO_2) and the SiO_2 (binder) in a sol–gel form. In accordance with this optimum, the powder of TiO_2 (P-25) was dispersed in a TEOS solution at a concentration of 40 $mg_{TIO_2}\ ml^{-1}_{SIO_2}$. Then, using the dip-coating method, thin films of mixture were applied to foams pre-covered by layers of SiO_2. The film of SiO_2/TiO_2 thus obtained was dried at 373 K and calcined at 675 K. This coating process was repeated five times [14].

2.3. Characterization

The coating rate was determined by image analysis [7]. The photographs obtained with a scanning electron microscope showed that the deposits of TiO_2/SiO_2 were laid down as successive layers. The images were treated so as to display the fraction of each surface corresponding to the film of TiO_2 deposited with each individual layer. In Table 1 the result shows that a complete coverage of the surface is reached after five deposits.

The optical properties of the supports and the suspensions were ascertained using an experimental optical set-up. The light was supplied by a source simulating the solar radiation ($1000\,W\,m^{-2}$, solar spectrum AM1.5). A support was used for positioning the material at the inlet of the integrating sphere, making possible the collection of the direct radiation as well as the scattered radiation transmitted [15]. The measurement was done by coupling an integrating sphere and a 1240 Shimadzu UV spectrophotometer (wavelength ranging from 250 to 1100 nm). The measurement of the transmission of light by each material gave the material absorbency at a given concentration and thickness. This method

Table 1
Coating ratio of TiO_2 on the surface of the foam according to the number of layers of TiO_2/SiO_2.

TiO_2 layers	0	1	2	3	4	5	7
Coating ratio	0	0.016	0.112	0.384	0.816	0.88	0.93

Table 2
Optical and kinetic properties of the materials used: absorbency (A), extinction coefficient (ε: l/g cm), slope of the kinetic constant versus intensity ($k_{Material}$: $m^2/W\,s$), apparent quantum yield (η_m: molecules per photon) and optical yield (η_o).

	Absorbency	Kinetic constant k (I)	Apparent quantum yield (η_m)	Optical yield (η_o)
Cellulosic material (2D)	1	0.048	0.0032	0.91
Suspension (P25)	0.9	0.178	0.0294	0.81
Foam (3D)	0.58	0.082	0.0106	0.53

is used by Cassano and Alfano [15] in the case of a P25 powder suspension. For the catalyst in powdered form, it was put in suspension at different concentrations and thicknesses. Then the quartz container holding the catalyst in suspension was placed on the experimental optical set-up. By measuring the transmission by the suspension at different concentrations of TiO_2, the correlation can be determined between the absorbance, the concentration of TiO_2 and the thickness of the container. For the foam, the measurements of transmission were done for various thicknesses of the material. These optical measurements enabled us to determine the optimal concentration and thickness of these two materials (Table 2).

2.4. Experimental photocatalytic set-up

A schematic diagram of the system is shown in Fig. 3 and was previously detailed [16]. The reactor was a cylindrical borosilicate glass tube (internal diameter 9 mm, wall thickness 1.5 mm) operated in a recirculation batch mode. In the case of the experimentation performed with the Ahlstrom material, it was fixed in a tube (diameter 5 mm) positioned at the axial center of the reactor. 2,4-DCP solution flowed through the reactor inside the annular space formed between the inner tube and the reactor inside wall and was mixed in the recirculation tank. 2,4-DCP solution was continuously re-circulated at different fixed rates, by means of a volumetric pump. This inner tube was kept for experiments with the Degussa P25 suspension. The radiation source was a UV lamp at 365 nm (VL-330). The length of the selected lamp made possible almost uniform intensity of radiation along the reactor axis. After calibration with a 365 nm UV sensor (UVA 365 from Lutron Electronic Enterprise), the radiation flux at the reactor axis was set between 0 and 50 W m^{-2}, the range of values corresponding to solar ultraviolet radiation. According to the literature [17], it is possible to deduce the average number of photons equivalent to radiation emitted at a range of wavelengths. In the ultraviolet wavelength range (280–400 nm) the flux of photons equal to 7.34×10^{19} photons $s^{-1}\,m^{-2}$ was calculated from the spectral distribution of the light source emitting at 50 W m^{-2}. To illuminate the total surface of the reactor an aluminium compound parabolic collector (CPC) was positioned just behind the reactor (Fig. 3b). Thanks to the design of the CPC reflector, the UV radiation is more or less uniformly distributed around the entire surface of the tubular reactor (front and back) [18]. Temperature inside the chamber containing the system was kept almost constant by means of a fan blowing the warm air out. During the experiment, the pH value was monitored, samples (10 ml) were taken out periodically and the mineralization of 2,4-DCP was monitored with a TOC-meter. The TOC meter used in the laboratory (SHIMADZU TOC-V CSH) is a device for measuring the carbon present in solution. Total carbon was determined by measuring the CO_2 formed when the sample was burnt at 680 °C in the presence of pure air flowing at a rate of 150 ml min^{-1}. This measurement was done using infrared spectrometry. The calibration of the COT meter was carried out with a solution of potassium hydrogen phthalate for the measurement of total carbon and, for inorganic carbon, with a solution of hydrogenate sodium carbonate.

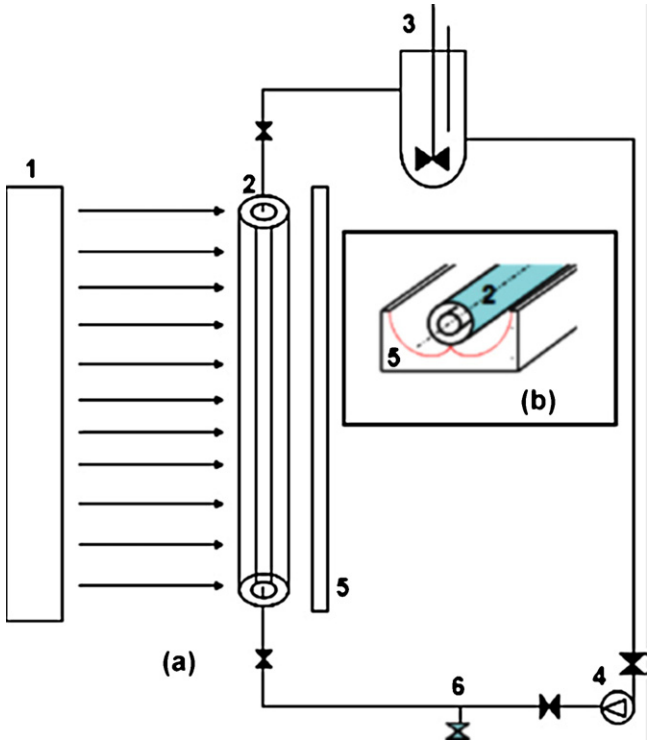

Fig. 3. (a) Experimental set up for the measurements of 2,4-DCP mineralization kinetic: (1) UV lamp 96 mm in height; (2) annular reactor; (3) container of samples stirred during the experiment; (4) volumetric pump; (5) compound parabolic collector (CPC); (6) bleed sample; (b) schematic view of the reactor and the collector.

3. Photocatalytic kinetics

The measurement of the kinetics of degradation was carried out on the target molecule, 2,4-DCP at an initial concentration of 20 mg l^{-1}. 1000 ml of the standardized solution was poured into a 2 l reactor and stirred continuously. The results were treated using a first order kinetic law based on TOC concentration. Concentration profiles as a function of time made it possible to deduce the kinetic constant k characterizing the material (Eq. (1)).

$$\frac{C_{TOC}}{C_{TOC_0}} = \exp(-kt) \quad (1)$$

C_{TOC_0} is the initial concentration of TOC in the reactor (mg l^{-1}), C_{TOC} is the concentration of TOC in the reactor (mg l^{-1}), k is the kinetic constant for photodegradation (s^{-1}), and t is the duration of irradiation (s).

Different flow rates (0.3, 0.85 and 1.5 l min^{-1}) were applied, corresponding respectively to the Reynolds numbers of 460, 1300 and 2300. The three support materials were subjected to radiation between 3 and 40 $W_{UV}\,m^{-2}$. In this range of experimental conditions, the photocatalytic kinetics of the degradation in TOC does not depend on the flow rate [16] and the consequence is that the mass transfer is not a limiting factor.

Vione et al. [19] has shown the possible effect of photolysis during the photo-degradation of 2,4-DCP due to the superposition of the spectrum of solar radiation and that of 2,4-DCP. On this account, the breaking down of the targeted molecule by photolysis was assessed in various conditions of radiation. In agreements with published results and depending on the intensity of the radiation (Fig. 4), photolysis specifically breaks down 2,4-DCP. The decrease in TOC corresponded to the mineralization of the pollutant into CO_2 and H_2O and showed that photolysis only partially affected the by-products resulting from the degradation of the targeted molecule. This was further indicated by an only slight variation in the

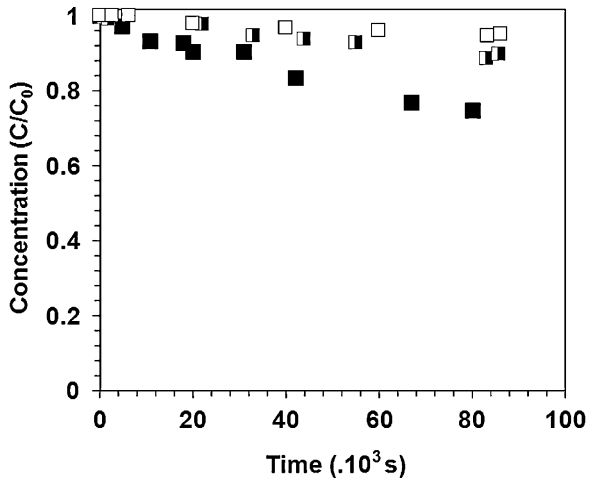

Fig. 4. Kinetics of the photolysis of 2,4-DCP carried out at different radiation strengths. The concentration, compared to the initial concentration, is given in TOC and the intensities applied were 3 (□), 20 (◨) and 40 (■) W m^{-2}.

concentration of TOC (<20%) observed after 24 h of radiation at 40 W_{UV} m^{-2} [20–23].

In order to establish the correlation between the structure of a material and its ability to degrade a pollutant, it is essential to know the effect of the radiation on the material involved. Fig. 5 shows, in the case of the Alhstrom material (2D materials), the kinetics of TOC photodegradation at given intensities. As the intensity of the light diminished, so did the kinetics of photodegradation slow down. The process is thus restricted by the amount of radiation received [7].

As to the catalyst in suspension, the kinetics of the photodegradation of the pollutant were observed for different concentrations of TiO_2 in order to determine which one produced the highest level of photocatalytic activity. The kinetic constants of photodegradation (k) obtained experimentally with the laboratory-scale reactor are shown in Fig. 6. The constants increased with the concentration of TiO_2, until a level close to 4 g l^{-1}. These values were then compared to the optical measurements indicating the optimal concentration of the catalyst, that is to say the concentration permitting the total absorption of the radiation entering the tubular reactor (thickness = 0.2 cm, $A_{TIO_2} = 0.9$). The optimal concentration

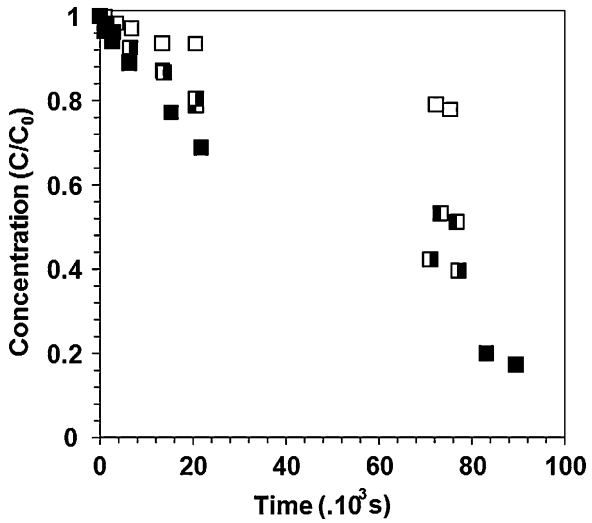

Fig. 5. Kinetics of the photocatalysis of 2,4-DCP carried out with cellulose material at different radiation strengths. The concentration, compared to the initial concentration, is given in TOC and the intensities applied were: 3 (□), 10 (◧), 20 (◨) and 40 (■) W m^{-2}.

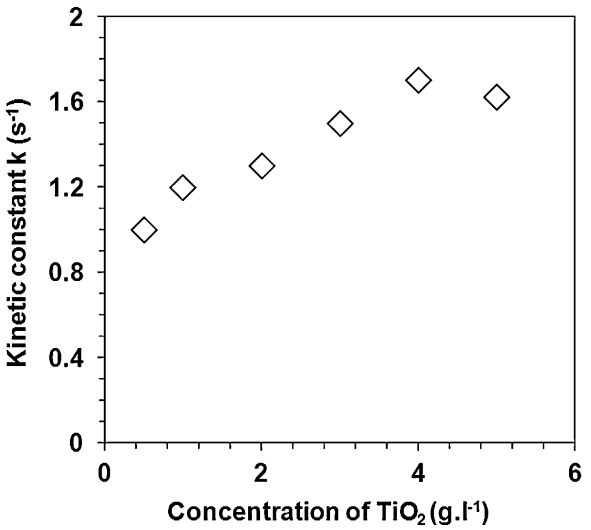

Fig. 6. Variation in the kinetic constant as a function of the concentration of the TiO_2 catalyst. The kinetic constants of mineralization have been deduced by relation no. 2.

observed was 4 g l^{-1}. It is thus clear that this method of determining the optimal concentration of TiO_2 is coherent with the measurement of the kinetics.

Fig. 7 reports the kinetics of photodegradation obtained with the foam scaffold and the suspension (at the optimal concentration). Whatever the material used (Figs. 5–7), the kinetics of photodegradation are that much the faster as the intensity of the irradiation is greater. The kinetic constants, derived from the kinetics of photodegradation, are given in Fig. 8 as a function of the intensity applied. Irrespective of the material used, the kinetic constants of photodegradation are correlated in a linear fashion with the intensity of the radiation. It is also apparent that the speed of degradation depends on the material used and is thus correlated to the structure of the material (Table 2).

The kinetic constants obtained with the TiO_2-coated foam were less than that of the suspension, by a factor of two in the best case but two times as great as that of the 2D material. As reported in the literature, the catalytic suspension showed a higher kinetic constant compared to supported photocatalytic materials. The 2D

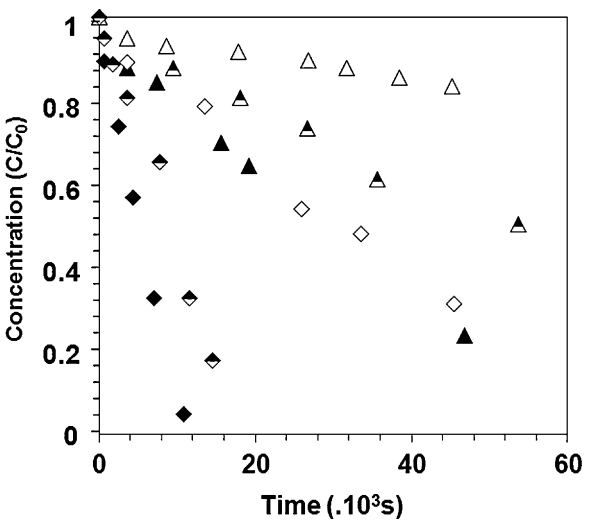

Fig. 7. Kinetics of the photocatalysis of 2,4-DCP carried out with the foam material (△) and the suspension (◊) at different radiation strengths. The concentration, compared to the initial concentration, is given in TOC and the intensities applied were: 3 (◊), 20 (◆) and 40 (⧫) W m^{-2}.

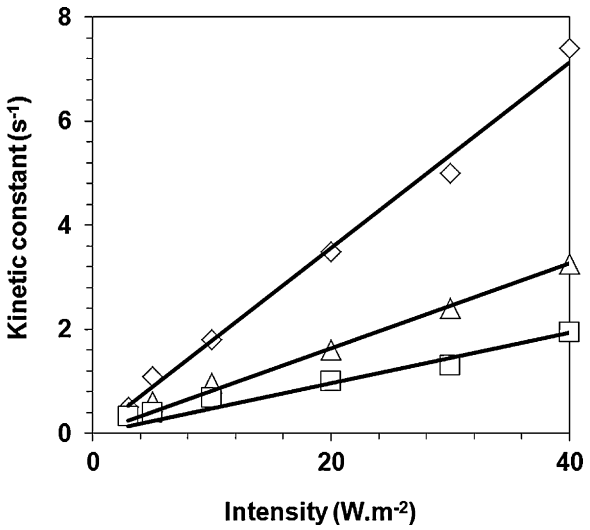

Fig. 8. Variation in the kinetic constant as a function of the intensity. The kinetic constants of mineralization have been deduced by relation no. 2 for the three materials: the catalyst in suspension (◊), the cellulose material (□) and the coated foam material (△).

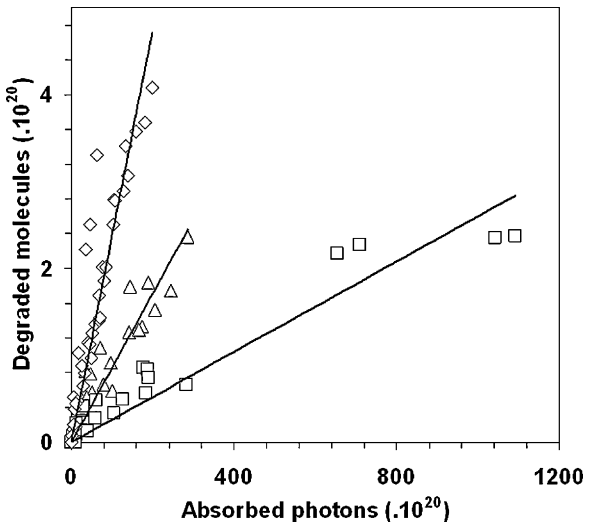

Fig. 10. Variation in the number of molecules degraded as a function of the number of photons absorbed by the material. The catalyst in suspension (◊), the cellulose material (□) and the coated foam material (△), have been represented by separate lines.

material was probably limited by its insufficient exchange interface. The powder in suspension represents the best option on the basis of the kinetic criterion. The TiO_2-coated foam offers an interesting alternative as a photocatalytic material.

4. Results and discussion

The quantum yield (η_p) is based on the photoconverted molecules divided by the absorbed photons [16,24]. The photoconverted molecules were deduced from the kinetics of 2,4-DCP mineralization. The photons absorbed were given by the number of photons received in the process. However, this quantity characterizes the efficiency of the process by integrating both the optical yield related to the reactor design and the yield due to the ability of a material to break down a molecule. The optical yield, which indicates the actual quantity of photons reaching the surface of the material, is obtained by considering the transfer of the radiation through the various components making up the equipment (Fig. 9). Three parts or factors were identified as impacting on the overall optical yield (η): (1) the CPC receptor which collects the radiation; (2) the borosilicate wall of the reactor which transmits the rays to the core of the reactor; and (3) the ability of the material to harness the radiation.

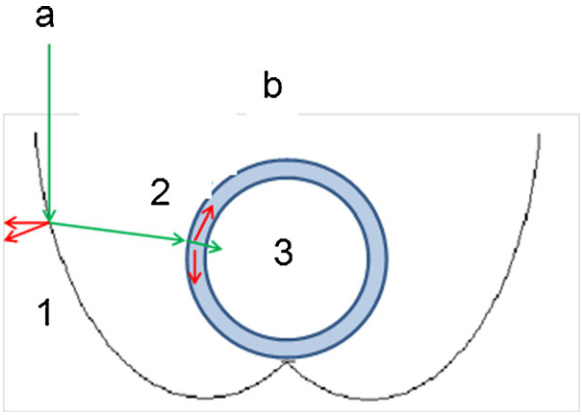

Fig. 9. Schematic view of the incident ray (a) and the reactor (b): (1) compound parabolic collector; (2) annular reactor; (3) photocatalytic material.

$$\eta_p = \eta_o.\eta_m$$

With $\eta_o = R{\cdot}T{\cdot}A$, η_p: apparent quantum yield of the process [23], η_m: apparent quantum yield of the material used [16], η_o: optical yield of the process, R: reflectivity of the CPC receptor, T: transmission from the reactor wall, A: absorbance of the material used.

The reflectivity of the CPC receptor and the transmission from the reactor wall were determined using optical measuring equipment. Reflectivity and transmission were 0.95 of the UV wavelength. As described previously, the concentration of TiO_2 at $4\,g\,l^{-1}$ was chosen in order to ensure almost total absorption of the radiation by the suspension ($A_{TiO_2} = 0.99$). Absorption by the foam was measured using the optical measuring equipment ($A_{Foam} = 0.58$). The material supplied by Alhstrom was a 2D material ($A_{Material} = 1$).

To compare the different materials used under identical radiation, we assessed their apparent quantum yields (η_m) which reflect the ability of these materials to degrade a pollutant when the same quantity of UV light is absorbed by each material. Fig. 10 shows the experimental variation in the number of molecules mineralized as a function of the number of photons actually absorbed on the surface of each material for all the levels of intensity applied. The quantity of molecules broken down was deduced from the kinetics of mineralization. Given that our TOC measurements correspond to the amount of carbon present in a solution, the kinetics of degradation in TOC reflect the breaking of the carbon–carbon link. The number of photons absorbed by each material tested was ascertained by the number of photons received divided by the optical yield (η_o). Despite the spread of the experimental results recorded at all intensities, the values obtained one straight line corresponding to the apparent quantum yield of each material (Table 2). This yield depends in a linear way on the quantity of photons absorbed irrespective of the intensity of the radiation received. Note also that the catalyst in suspension was more effective than the other two coated materials. In fact, the ability of the catalyst in suspension to use the radiation was almost three times greater than that of the foam and just about ten times greater than that of the 2D cellulose material. Marugan, who worked on the kinetics of breaking the link in methanol using a catalyst in suspension [25,26], obtained an apparent quantum yield comparable to our experimental results. Such

yields reflect the ability of the materials involved to effectively use the radiation to break down links. Therefore materials that ensure an even distribution of the catalyst throughout the reactor volume, whether they are based on suspension or supports, significantly enhance the process's efficiency.

5. Conclusion

Efficient materials able to provide a highly active specific surface area per unit volume of reactor, such as a foam and the suspension, were used. The supports used, differing in the form they took (powder, 2D and foam), together highlighted the importance of a material's structure on its capacity to utilize the radiation. At a given level of irradiation, the apparent quantum yield of the 2D material revealed that this support does not use very efficiently the input of light that it absorbs. In fact, the apparent quantum yield of the 2D substrate was several times lower than that of the suspension. In contrast, it is noteworthy that the apparent quantum yield of the foam tended towards that observed for suspensions which form the ideal support thanks to their optimal ability to harness the light. It thus emerges that the rate of degradation is related exclusively to the quantity of light absorbed and utilized by the each material. For each material, the efficiency of the material was independent of the intensity of the radiation received. Consequently, it tends to demonstrate that the design of a photocatalysis process can be determined on the basis of a precise estimate of the solar radiation input, irrespective of its strength. In this context, macroporous reticulated materials such as foams show promise as supports for photocatalysts. Furthermore, modifications to their architecture (mesh density) ensure control of the harnessing of the radiation received for a given volume [7].

References

[1] J.B. Galvez, S. Malato, Solar Detoxification, United Nations Educational, Scientific and Cultural Organization, 2003.
[2] D. Bahnemann, Photocatalytic water treatment: solar energy applications, Sol. Energy 77 (2004) 445–459.
[3] A.G. Agrios, P. Pichat, State of the art and perspectives on materials and applications of photocatalysis over TiO_2, Rev. Appl. Electrochem. 58 (2005) 655–663.
[4] A.O. Ibhadon, G.M. Grennway, Y. Yue, P. Falaras, D. Tsoukleris, The photocatalytic activity and kinetics of the degradation of an anionic azo-dye in a UV irradiated porous titanio foam, Appl. Catal. B: Environ. 84 (2008) 351–355.
[5] S. Josset, S. Hajiesmaili, D. Begin, D. Edouard, C. Pham-Huu, M.C. Lett, N. Keller, V. Keller, UV-A photocatalytic treatment of *Legionella pneumophila* bacteria contaminated airflows through three-dimensional solid foam structured photocatalytic reactor, J. Hazard. Mater. 175 (2010) 372–381.
[6] J. Taranto, D. Frochot, P. Pichat, Photocatalytic air purification: comparative efficacy and pressure drop of a TiO_2-coated thin mesh and a honeycomb monolith at high air velocities using a 0.4 m^3 close-loop reactor, Sep. Purif. Technol. 67 (2009) 187–193.
[7] G. Plantard, V. Goetz, D. Sacco, TiO_2-coated foams as a medium for solar catalysis, Mater. Res. Bull. 46 (2010) 231–234.
[8] I.J. Ochuma, O.O. Osibo, R.P. Fishwick, S. Pollington, A. wagland, J. Wood, J. Winterbottom, Three-phase photocatalysis using suspended titania and titania supported on a reticulated foam monolith for water purification, Catal. Today 128 (2007) 100–107.
[9] G. Plesh, M. Gorbar, U. Vogt, K. Jesenak, M. Vargova, Reticulated macroporous ceramic foam supported TiO_2 for photocatalytic applications, Mater. Lett. 63 (2009) 461–463.
[10] M. Addamo, Photocatalytic thin film of TiO_2 by sol-gel process using titanium tetraisopropoxide as the precursor, Thin Solid Films 516 (2008) 3802–3807.
[11] R.A. Doong, R.A. Maithreepala, S.M. Chang, Heterogeneous and homogeneous photocatalytic degradation of chlorophenols in aqueous titanium dioxide and ferrous ion, Water Sci. Technol. 42 (2000) 253–260.
[12] J. Aguado, R. Van Grieken, M.J. Lopez-Munoz, J. Marugan, A comprehensive study of the synthesis, characterization and activity of TiO_2 and mixed TiO_2/SiO_2 photocatalyst, Appl. Catal. A: Gen. 312 (2006) 202–212.
[13] R. Enrique, B. Beaugiraud, P. Pichat, Mechanistic implications of the effect of TiO_2 accessibility in TiO_2–SiO_2 coatings upon chlorinated organics photocatalytic removal in water, Water Sci. Technol. 49 (2004) 147–152.
[14] G. Plantard, V. Goetz, F. Correia, J.P. Cambon, Importance of a medium's structure on photocatalysis: using TiO_2-coated foams, Sol. Energy Mater. Sol. Cells (2011) (under proof).
[15] A. Cassano, O.M. Alfano, Reaction engineering of suspended solid heterogeneous photocatalytic reactors, Catal. Today 58 (2000) 167–197.
[16] V. Goetz, J.P. Cambon, D. Sacco, G. Plantard, Modeling aqueous heterogeneous photocatalytic degradation of organic pollutants with immobilized TiO_2, Chem. Eng. Process.: Process Intensification 48 (2009) 532–537.
[17] N. Peill, M. Hoffmann, Development and optimization of a TiO_2-coated fiber cable reactor: photocatalytic degradation of 4-chlorophenol, Environ. Sci. Technol. 29 (1995) 2974–2981.
[18] S. Malato, J. Blanco, A. Vidal, C. Richter, Photocatalysis with solar energy at a pilot-plant scale: an overview, Appl. Catal. B: Environ. 37 (2002) 1–15.
[19] D. Vione, C. Minero, F. Housari, S. Chiron, Photoinduced transformation processes of 2,4-dichlorophenol and 2,6-dichlorophenol on nitrate irradiation, Chemosphere 69 (2007) 1548–1554.
[20] B. Bayarri, M.N. Abellàn, J. Gimenez, S. Esplugas, Study of the wavelength effect in the photolysis and heterogeneous photocatalysis, Catal. Today 129 (2007) 231–239.
[21] F. Al Momani, C. Sans, S. Esplugas, A comparative study of the oxidation of 2.4 dichlorophenol, J. Hazard. Mater. B 107 (2004) 123–129.
[22] B. Bayarri, J. Giménez, D. Curco, S. Esplugas, Photocatalytic degradation of 2.4 dichlorophenol by TiO_2/UV: kinetics, actinometries and models, Catal. Today 101 (2005) 227–236.
[23] J. Gimenez, D. Curco, M.A. Queral, Photocatalytic treatment of phenol and 2.4 dichlorophenol in a solar plant in the way to scale up, Catal. Today 54 (1999) 229–243.
[24] H. Lasa, B. Serrano, M. Salaices, Photocatalytic Reaction Engineering, Springer, 2005.
[25] J. Marugan, D. Hufschmidt, M.J. Lopez-Munoz, V. Selzer, D. Bahnemann, Photonic efficiency for methanol photooxidation and hydroxyl radical generation on silica-supported TiO_2 photocatalyst, Appl. Catal. B: Environ. 62 (2006) 201–207.
[26] C.Y. Wang, J. Rabani, D. Bahnemann, B. Dohrmann, Photonic efficiency and quantum yield of formaldehyde formation from methanol in the presence of various TiO_2 photocatalysts, J. Photochem. Photobiol. A 148 (2002) 169–176.